Volume 57(9): 811–824, 2009
Journal of Histochemistry & Cytochemistry
http://www.jhc.org

ARTICLE

Endocrine Cell Clustering During Human Pancreas Development

Jongmin Jeon,[1] Mayrin Correa-Medina,[1] Camillo Ricordi, Helena Edlund, and Juan A. Diez

Diabetes Research Institute, University of Miami Leonard M. Miller School of Medicine, Miami, Florida (JJ,MC-M,CR,JAD), and Umeå Center for Molecular Medicine, Umeå University, Umeå, Sweden (HE)

SUMMARY The development of efficient, reproducible protocols for directed in vitro differentiation of human embryonic stem (hES) cells into insulin-producing β cells will benefit greatly from increased knowledge regarding the spatiotemporal expression profile of key instructive factors involved in human endocrine cell generation. Human fetal pancreases 7 to 21 weeks of gestational age, were collected following consent immediately after pregnancy termination and processed for immunostaining, in situ hybridization, and real-time RT-PCR expression analyses. Islet-like structures appear from approximately week 12 and, unlike the mixed architecture observed in adult islets, fetal islets are initially formed predominantly by aggregated insulin- or glucagon-expressing cells. The period studied (7–22 weeks) coincides with a decrease in the proliferation and an increase in the differentiation of the progenitor cells, the initiation of *NGN3* expression, and the appearance of differentiated endocrine cells. The present study provides a detailed characterization of islet formation and expression profiles of key intrinsic and extrinsic factors during human pancreas development. This information is beneficial for the development of efficient protocols that will allow guided in vitro differentiation of hES cells into insulin-producing cells.
(J Histochem Cytochem 57:811–824, 2009)

KEY WORDS
fetal pancreas
gene expression profile
human
immunohistochemistry
islet formation

THE PROSPECT of successful cell replacement therapies for treatment of diabetes will require: (1) the development of improved strategies for immune tolerance in the recipients, and (2) efficient and stable in vitro differentiation protocols that reproducibly will allow the generation of functional, insulin-producing β cells from human embryonic stem (hES) cells. To achieve the latter, a detailed knowledge about the factors that at different levels control pancreatic cell specification, differentiation, and proliferation, and the formation of mature islets, including the morphological process and interactions among the different endocrine cells, is likely to be critical. Our current molecular understanding of pancreatic development originates, however, predominantly from studies of mouse pancreatic development, where genetic approaches have identified both intrinsic and extrinsic factors that operate at different levels of pancreatic development (Edlund 2002; Bonal and Herrera 2008; Oliver-Krasinski and Stoffers 2008). These data have frequently been extrapolated to human pancreatic development. Human pancreatic developmental processes may, however, differ from those of the mouse. Although the basic developmental program may be similar, the identity and/or timing of activity of some factors may be critically different. Detailed characterization of human fetal pancreatic development will provide information regarding the spatiotemporal expression of intrinsic and extrinsic factors that are likely to govern important aspects of human pancreatic development.

During fetal development, the human pancreas forms from a dorsal and a ventral protrusion of the primitive gut epithelium. On day 26, the dorsal pancreatic bud grows into the dorsal mesentery and over the next few days, the ventral bud sprouts into the ventral mesentery. Late in the sixth week, the pancreatic buds fuse to form the definitive pancreas, and their ductal systems become interconnected. On a molecular and cellular level, the formation of the mouse endocrine pancreas is divided into several steps, including: pancreatic fate specification, characterized by the coexpression of *Ipf1* and *Ptf1a*; proliferation of the pancreatic progenitor cells, which is controlled in part by NOTCH,

Correspondence to: Juan Diez, Diabetes Research Institute, University of Miami Leonard M. Miller School of Medicine, 1450 NW 10th Avenue (R-134), Miami, FL 33136. E-mail: jdiez@med.miami.edu
[1]These authors contributed equally to this work.
Received for publication November 24, 2008; accepted April 2, 2009 [DOI: 10.1369/jhc.2009.953307].

0022-1554/09/$3.30

fibroblast growth factor (FGF), and epidermal growth factor (EGF) signaling; endocrine cell fate determination as a result of transient expression of *Ngn3* in the proendocrine cells; and differentiation and maturation of the endocrine progenitor cells into functional endocrine cells, including glucose-responsive β cells, as a result of the expression of distinct transcription factors such as *Arx*, *Pax4*, *Ipf1*, *Nkx2-2*, *Nkx6-1*, *Mafa*, *Mafb*, *Neurod1*, *Pax6*, and *Isl1* (reviewed in Edlund 1998, 1999,2002; Bonal and Herrera 2008; Oliver-Krasinski and Stoffers 2008).

Although previous studies have described the expression of some endocrine hormones and transcription factors during human fetal pancreas development (Polak et al. 2000; Piper et al. 2004; Lyttle et al. 2008; Sarkar et al. 2008), a detailed and longitudinal expression profile of the main endocrine markers, combined with a thorough morphological study of islet formation, may expand our understanding of human endocrine pancreas formation. In the present study, we present data on the morphological pattern by which islet-like structures form during human pancreatic development. We also analyze, by quantitative real-time (qRT)-PCR, in situ hybridization, and immunohistochemistry, the gene expression profile of selected candidate intrinsic and extrinsic factors in human fetal pancreas from 7 to 22 weeks of gestational age. We herein describe the temporal expression profiles of these factors. The results presented here may help to determine the sequential activity of the key developmental factors behind the morphological changes occurring during islet clustering.

Materials and Methods

Human Tissue

Human fetal pancreases were collected from fetal tissue fragments immediately after elective termination of pregnancy performed by aspiration between 7 to 21 weeks of development, in compliance with US legislation and the guidelines of our institution. Gestational age was determined on the basis of time since the last menstrual period and the measured crown–rump length and biparietal diameter by ultrasonography. The isolated tissues were processed directly after extraction, with less than 8 hr of cold ischemia time. Tissues were transferred in ice-cold PBS, pH 7.4, for immunohistochemical analysis, or in RNAlater solution (Ambion; Austin, TX) for RT-PCR analysis. Human pancreas tissue from two adults, ages 53 and 54 years (obtained from the human islet cell processing facility at the Diabetes Research Institute, University of Miami), were also used. The numbers of cases for each experiment are listed in Table 1.

Immunostaining

Tissues were fixed in 4% paraformaldehyde (w/v) at 4C for 15 hr, followed by PBS washing for 1 min, and then stabilized in 30% sucrose (w/v) in PBS at 4C overnight. The tissues were mounted in Tissue-Tek OCT compound (Sakura Finetek; Torrance, CA) and stored at −80C. Five-μm sections were cut, air-dried on precleaned superfrost microslides (VWR Scientific; West Chester, PA), and used immediately or stored at −80C. The frozen slides were thawed at room temperature for 30 min and washed in 0.1% (v/v) Triton X-100 (USB; Cleveland, OH)-TBS (Santa Cruz Biotechnology, Inc.; Santa Cruz, CA) (TBS-T) three times for 5 min each. Sections were blocked in 10% (v/v) fetal bovine serum (FBS) in TBS-T at room temperature for 20 min. Primary and secondary antibodies were diluted in 10% FBS in TBS-T. Primary antibodies were incubated at 4C overnight or at room temperature for 1 hr (anti-hormone antibodies) and secondary antibodies at 4C or room temperature for 1 hr. The following primary antibodies and dilutions were used: mouse anti-insulin (1:1000; Sigma, St. Louis, MO); guinea pig anti-glucagon (1:1000; Linco Research Inc., St. Charles, MO); rabbit anti-IPF1 (1:8000; generated against a keyhole limpet hemocyanin (KLH)-conjugated peptide of human IPF1 by Agrisera Ab, Vännäs, Sweden); rabbit anti-Isl1 (1:250; generated against a KLH-conjugated peptide of human Isl1 by Agrisera Ab); mouse anti-human E-cadherin (10 μg/ml; Zymed, South San Francisco, CA); mouse anti-human nestin (1:200; Chemicon, Billerica, MA); rabbit anti-somatostatin (1:500; Dako, Carpinteria, CA); rabbit anti-pancreatic polypeptide (1:1000; Dako); and rabbit anti-Ki67 (1:50; Zymed). Secondary antibodies used were: Alexa Fluor 488–conjugated goat anti-rabbit (1:400; Molecular Probes, Carlsbad, CA); Alexa Fluor 568–conjugated goat anti–guinea pig (1:400; Molecular Probes); and Alexa Fluor 647–conjugated goat anti-mouse (1:400; Molecular Probes). 4,6-Diamidino-2-phenylindole, dihydrochloride (12.5 μg/ml; Invitrogen, Carlsbad, CA) was used as nuclear counterstaining. Image acquisition was performed using a Zeiss LSM510 confocal microscope (Carl Zeiss; Jena, Germany). Negative control assays were performed without primary antibodies.

Table 1 Summary of cases

	Gestational age (weeks)																
	7	8	9	10	11	12	13	14	15	16	17	18	19	20	21	22	Total
No. of cases for PCR analysis	1	3	3	3	3	3	3	3	2	1	2	4	1	1	3	0	36
No. of cases for immunostaining	0	4	3	3	4	4	4	4	2	1	2	3	1	1	3	1	40

Immunohistochemical Analyses

To quantify images, the optical thicknesses of the two channels were equalized prior to image acquisition. Raw confocal images (1024 × 1024 pixels, 12-bit data depth) were sequentially obtained with a Zeiss LSM510 with a 20×, 0.5 NA, plan-neofluar objective (Carl-Zeiss). Colocalization analysis was performed on 17 randomly selected raw confocal images of each case using a colocalization routine mode of the Zeiss LSM510 software (version 3.2). The colocalization coefficient, which is the ratio between the number of colocalizing pixels and the total number of pixels above the threshold, was used as a quantitative parameter, where 1 indicates the colocalization of all pixels, and 0 indicates no colocalization. The intensity of the pixels does not affect the calculation. First, the intensity background levels of images were automatically obtained by measuring the mean intensity of each local background stain outside the cells, using the image regions-of-interest mode. Second, the whole-image background thresholds were determined by subtracting the average local background intensity plus 2× standard deviation of each channel, and finally the software calculated a colocalization coefficient and the area/colocalized area for each channel. Quantification of images was repeated three times independently. The average values of all of the colocalization coefficients and the area of different samples were plotted.

To count α and β cells, four tissue sections per case ($n=3$) were randomly selected from pancreases at 9- and 10 weeks' gestational age. The numbers of insulin-expressing, glucagon-expressing, and coexpressing cells were manually counted through a fluorescent microscope. Average values of three independent experiments were plotted.

To measure the diameter of islet-like clusters, those bigger than 70 μm in diameter were selected for quantification in the 243 confocal images used. The size was manually measured by averaging the maximum and minimum diameters of each cluster containing more than ten cells expressing insulin, glucagon, or both, using the ruler toolbar in the Zeiss LSM510 software. Average values of three independent experiments were plotted. To analyze the percentage of separated clusters containing only glucagon- or insulin-expressing cells, we quantified only those aggregates bigger than 70 μm between 16 and 21 weeks, two or three cases per age, as described above.

To define the spatial distribution of islet-like clusters, all the tissue sections of pancreas tissues ($n=39$) used for the quantification of colocalization were analyzed using a Zeiss Axiovert 200 fluorescent microscope, and the 243 confocal images obtained were reviewed.

qRT-PCR

Total RNA was isolated from the sample tissues using the RNeasy Mini kit (Qiagen; Valencia, CA) according to the manufacturer's directions. Of total RNA, 0.5 μg was used for reverse transcription using the first-strand cDNA synthesis kit (Roche; Indianapolis, IN). PCR reactions were run using Taqman gene expression assays according to the manufacturer's directions (Applied Biosystems; Foster City, CA) in a 7900HT fast real-time PCR system (Applied Biosystems). We used low-density array cards (Applied Biosystems), designed in our laboratory, containing 48 genes. The primers used in this article are listed in Table 2; a complete list of the primers contained in the cards is available upon request. Relative quantification (RQ) of the gene expression was calculated based on the equation $RQ = 2^{-\Delta Ct}$, where ΔCt is the difference between the Ct value (number of cycles at which amplification for a gene reaches a threshold) of the target gene and the Ct value of the ubiquitous housekeeping gene *18S*. The data represent the mean ± SEM of one to three specimens (see Table 1).

In Situ Hybridization

In situ hybridization using a digoxigenin (DIG)-labeled *NGN3* probe was performed essentially as described (Obernosterer et al. 2007). A total of 30 ng of DIG-labeled *NGN3* probe was diluted in 150 μl of hybridization buffer, applied to the slides, and allowed to hybridize at 70C overnight. Slides were then washed for 1 hr in 0.2 × 150 mM sodium chloride and 15 mM sodium citrate buffer solution (Ambion-Applied Biosystems) and incubated with alkaline phosphatase-conjugated sheep anti-DIG antibody (1:2500; Roche) overnight at 4C. Alkaline phosphatase reaction was carried out in polyvinyl alcohol with 200 μl of $MgCl_2$ 1 M and 140 μl of nitroblue tetrazolium chloride/5-bromo-4-chloro-3-indolyl phosphate, toluidine salt stock (Roche) for 1–3 days. Hybridization with sense DIG-labeled *NGN3* probe was used as control.

Statistical Analysis

All data are presented as mean ± SEM.

Results

Ontogeny of Pancreatic Endocrine Cells in the Developing Human Pancreas

The appearance of endocrine cells in the developing human pancreas was determined by immunohistochemical analyses. At week 8, a few insulin-expressing cells, but not glucagon-expressing cells, were detectable (data not shown). At week 9, the first glucagon-positive cells emerged, although insulin-expressing cells were more abundant at this stage, and, in addition, occasional insulin/glucagon double-positive cells were observed (Figure 1A). A few somatostatin-expressing cells, but not pancreatic polypeptide (PP)-expressing cells, were observed at week 10 (data not shown), and by week 17, somatostatin-expressing cells were inter-

Table 2 Summary of primers

Gene abbreviation	Gene name	ABI Taqman assay no.
18S	Eukaryotic 18S rRNA	Hs99999901_s1
AMY	Amylase	Hs00420710_g1
ARX	Aristaless-related homeobox	Hs00292465_m1
BMP4	Bone morphogenetic protein 4	Hs00370078_m1
BMPR1A	Bone morphogenetic protein receptor, type IA	Hs01034909_g1
CA2	Carbonic anhydrase II	Hs00163869_m1
DLK1	Delta-like 1 homolog (Drosophila)	Hs00171584_m1
EGFR	Epidermal growth factor receptor	Hs00193306_m1
FGFR2	Fibroblast growth factor receptor 2	Hs00240796_m1
FOXA2	Forkhead box A2	Hs00232764_m1
FOXD3	Forkhead box D3	Hs00255287_s1
GCG	Glucagon	Hs00174967_m1
GCK	Glucokinase	Hs00175951_m1
GHRL	Ghrelin/obestatin preprohormone	Hs00175082_m1
HES1	Hairy and enhancer of split 1, (Drosophila)	Hs00172878_m1
HES5	Hairy and enhancer of split 5 (Drosophila)	Hs01387463_g1
HEY1	Hairy/enhancer-of-split related with YRPW motif 1	Hs00232618_m1
HLXB9	Homeobox HB9	Hs00232128_m1
IAPP	Islet amyloid polypeptide	Hs00169095_m1
ID2	Inhibitor of DNA binding 2, dominant negative helix-loop-helix protein	Hs00747379_m1
INS	Insulin	Hs02741908_m1
INSM1	Insulinoma-associated 1	Hs00357871_s1
IPF1	Insulin promoter factor 1, homeodomain transcription factor	Hs00426216_m1
ISL1	ISL1 transcription factor, LIM/homeodomain, (islet-1)	Hs00158126_m1
MAFB	V-maf musculoaponeurotic fibrosarcoma oncogene homolog B	Hs00534343_s1
NEUROD1	Neurogenic differentiation 1	Hs00159598_m1
NEUROG3	Neurogenin 3	Hs00360700_g1
NKX2-2	NK2 transcription factor related, locus 2 (Drosophila)	Hs00159616_m1
NKX6-1	NK6 transcription factor related, locus 1 (Drosophila)	Hs00232355_m1
NOTCH1	Notch homolog 1, translocation-associated (Drosophila)	Hs00413187_m1
ONECUT1	One cut domain, family member 1	Hs00413554_m1
PAX4	Paired box gene 4	Hs00173014_m1
PCSK1	Proprotein convertase subtilisin/kexin type 1	Hs00175619_m1
PCSK2	Proprotein convertase subtilisin/kexin type 2	Hs00159922_m1
PTF1A	Pancreas specific transcription factor, 1a	Hs00603586_g1
SST	Somatostatin	Hs00356144_m1
TCF2	Transcription factor 2	Hs00172123_m1

spersed with glucagon-expressing cells at the periphery of the forming islet cell clusters. By week 17, a few PP cells were also observed at the periphery of the islet cell clusters (Figure 1B).

Between weeks 8 and 11, the distribution of endocrine cells was scattered, but by week 12, insulin and/or glucagon cells started to form small clusters; by week 14, these clusters were more prominent, with a core of insulin-positive cells surrounded by glucagon-positive cells (Figure 1A). By weeks 16–17, glucagon cells no longer formed a distinct ring of cells surrounding the insulin cells; instead, insulin and glucagon cells appeared to predominantly self-aggregate, and by week 18, distinct, albeit juxtaposed, insulin and glucagon cell clusters had formed. The analysis of these homotypic clusters revealed that they constitute 10% of the total clusters bigger than 70 μm at week 17, 62.5% at week 18, 33.3% at week 19, 33.3% at week 20, and 13.3% at week 21. This type of cluster was not detected before week 17.

By week 21, a few glucagon cells were detected within the clusters of insulin cells and vice versa. The clusters of insulin-positive cells contained fewer replicating cells, as revealed by Ki67 immunostaining, than the group of glucagon cells (Figure 1A). During development, the size of the islet-like structures increased to reach the maximum average diameter at 14 weeks, although occasional huge clusters of cells, some even bigger than adult islets, were observed (Figures 1A and 1C).

We next quantified the number of cells expressing glucagon and/or insulin-positive cells at 9 and 10 weeks, and the total area of glucagon- and insulin-positive cells in tissue sections from 8 to 21 weeks. At 9 and 10 weeks, most of the glucagon-positive cells coexpressed insulin (Figure 2B), although distinct insulin-only cells were clearly detectable at these stages (Figures 1A and 2A). Cells coexpressing insulin and glucagon were observed during the whole period studied (9 to 21 weeks), but they represented merely a small fraction of the total

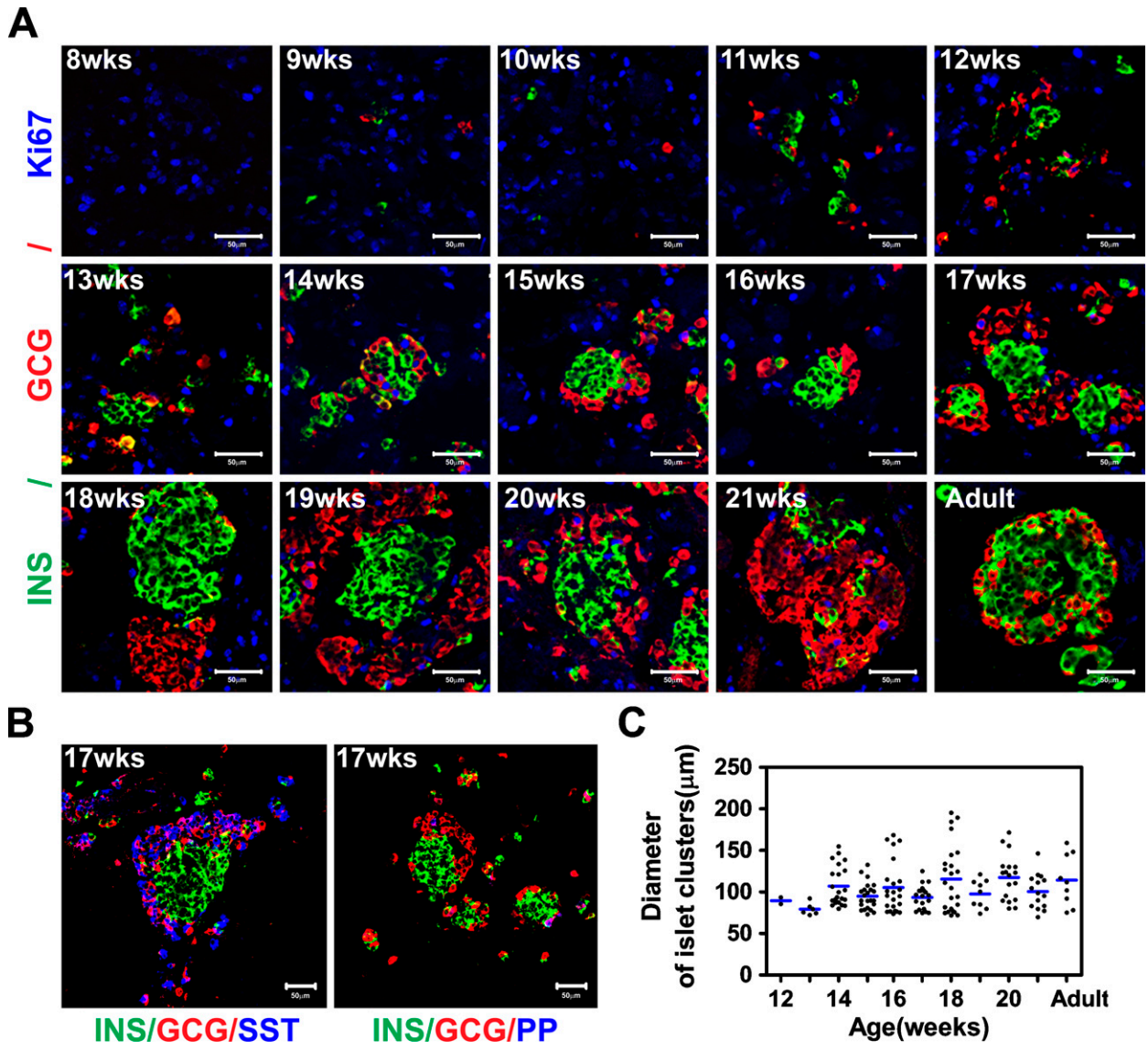

Figure 1 Endocrine cells clustering during human pancreas development. (**A**) Immunostaining of human fetal and adult pancreas with anti-insulin (green), anti-glucagon (red), and anti-Ki67 (blue) antibodies. Numbers in the image indicate the gestational age in weeks (wks). (**B**) Seventeen-week fetal pancreas immunostained with anti-insulin (green), anti-glucagon (red), and anti-somatostatin (blue) or pancreatic polypeptide (PP) (blue). INS, insulin; GCG, glucagon; SST, somatostatin. (**C**) Diameter measurement of islet-like clusters. Clusters ≥ 70 μm were counted, and the size values were plotted. The lines indicate the mean ± SEM of the average diameter of the clusters. Bar = 50 μm.

insulin- and glucagon-expressing cells (Figures 2C and 2D). When determining the colocalization index, i.e., the ratio between the double-positive cells and the total cells positive for glucagon or insulin, where 0 indicates only single-hormone expression and 1 complete co-expression, a fair proportion of the glucagon cells were shown to coexpress insulin until week 14 (Figure 2C).

After week 15, the percentage of double-positive cells is similar among the glucagon- or insulin-expressing cells (Figure 2C). Interestingly, the cells coexpressing insulin and glucagon after week 14 are mainly found in small aggregates and not in the big clusters (Figure 2A). The total area of insulin-positive cells increased rapidly from 8 to 14 weeks (Figure 2D). The total area of glucagon-positive cells also increased during this period, and from ~16 weeks, the areas of glucagon and insulin were similar (Figure 2D). These data show that although insulin-positive cells emerge slightly earlier than glucagon-positive cells during human pancreatic development, a near 1:1 ratio resembling that observed in adult human islets (Cabrera et al. 2006) is already observed at mid-gestation.

Next, we analyzed the spatial appearance of the islet-forming structures in the developing pancreas by screening for insulin and glucagon aggregates in the central and peripheral regions of the pancreas (Figure 3A).

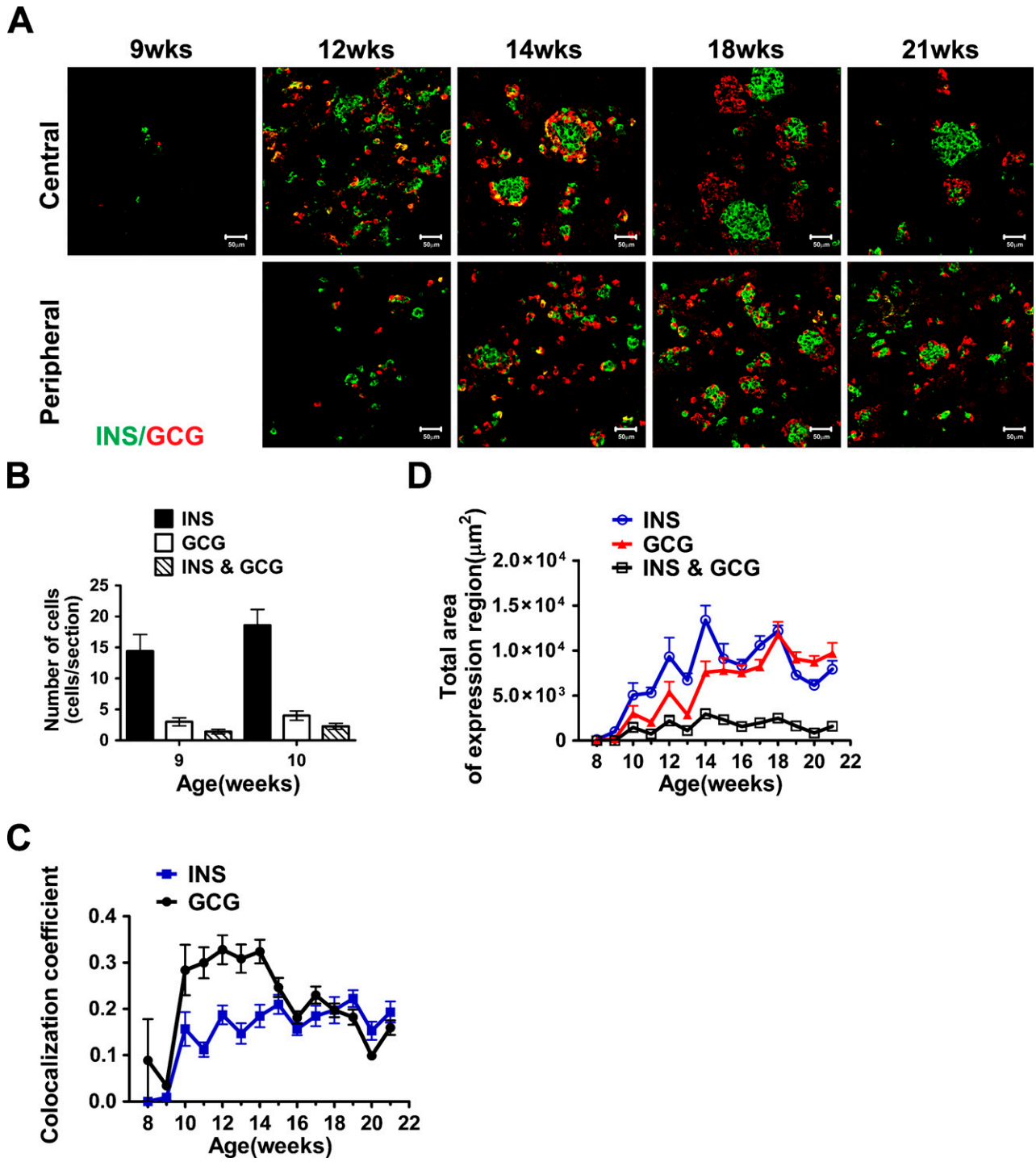

Figure 2 Coexpression of insulin and glucagon during human pancreas development. (**A**) Immunostaining of human fetal pancreas with anti-insulin (green) and anti-glucagon (red) antibodies. Cells coexpressing insulin and glucagon appear in yellow. Tissue sections were obtained from the central or peripheral areas of the fetal pancreas as indicated. Numbers indicate the gestational age in weeks (wks). Bar = 50 μm. (**B**) Quantification of the insulin, glucagon, or double-positive cells (as detected by immunostaining) in 9- and 10-week fetal pancreas. (**C**) Co-localization index for insulin and glucagon. Images of immunostained fetal pancreas, using anti-insulin and anti-glucagon antibodies, were analyzed. Values indicate the ratio between double- and single-stained cells. (**D**) Total area of insulin- or glucagon-expressing cells.

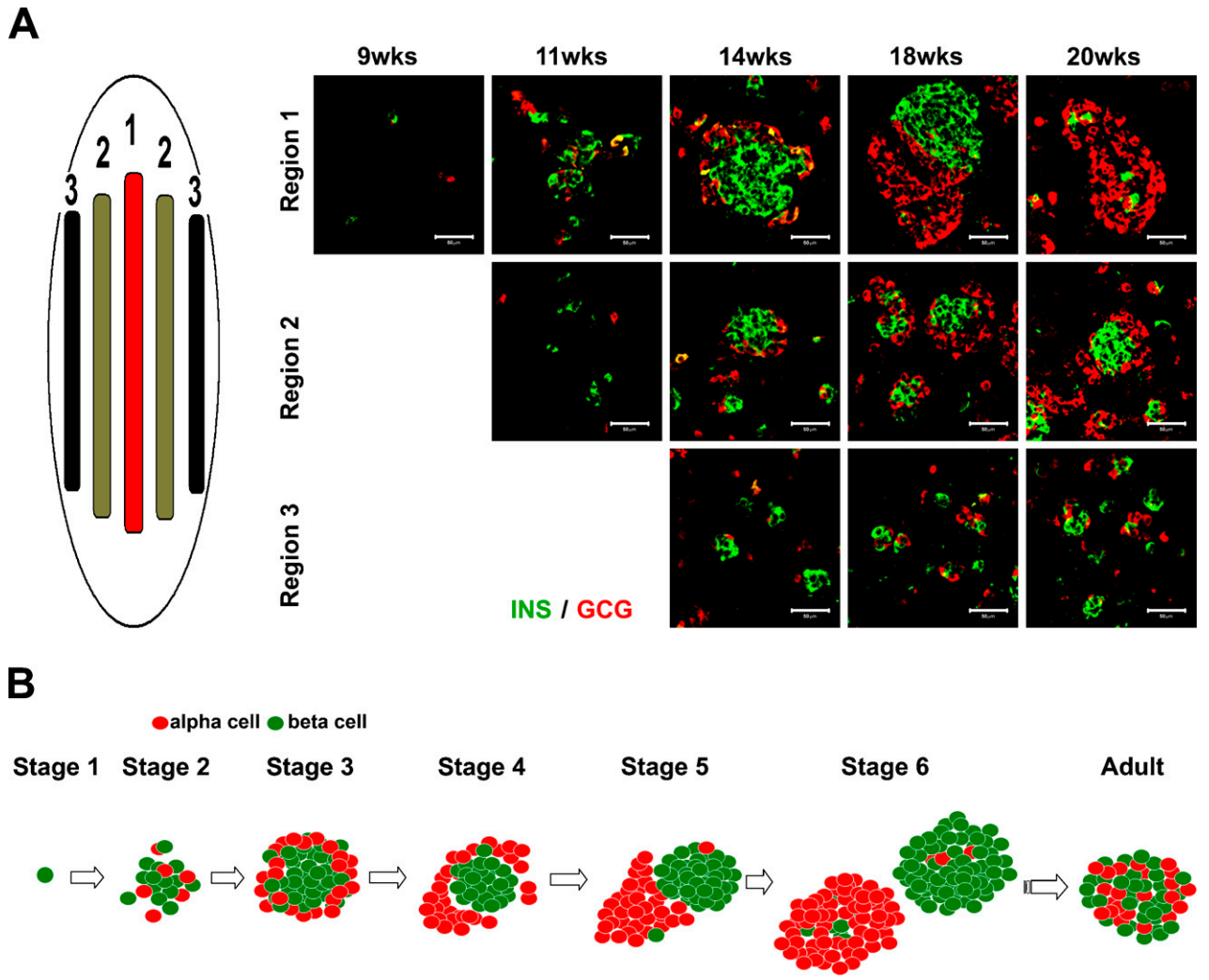

Figure 3 Spatial distribution of clustering endocrine cells. (**A**) Tissue sections were obtained from the center and the periphery of 9-, 11-, 14-, 18-, and 20-week gestational-age human pancreas and immunostained using anti-insulin (green) and anti-glucagon (red) antibodies. (**B**) Schematic drawing showing the different morphological phases during islet-like cluster formation. Bar = 50 μm.

The clustering of insulin and glucagon cells appeared to begin in the central region of the pancreas and then to spread to the periphery. At week 20, the insulin- and glucagon-positive cells thus appeared less aggregated in the periphery than in the center, even compared with earlier stages (Figure 3A). We must stress that at any given stage, the morphology of the endocrine cell clusters is a compilation of all the previous stages, co-existing single cells and small and big aggregates.

Clustering of Endocrine Cells Occurs Concomitantly With Increased Hormonal Expression

To determine the expression of transcription factors, we performed expression analyses using qRT-PCR, in situ hybridization, and immunostaining of human fetal pancreas between 7 and 21 weeks of gestational age. In mouse, the transcription factors *Ipf1* (also known as *Pdx1*), *Ptf1a*, and *Hlxb9* are expressed in early pancreatic progenitors, and their function is critical for pancreatic development (Jonsson et al. 1994; Offield et al. 1996; Edlund 1999,2001; Harrison et al. 1999; Li et al. 1999). All these genes have additional late functions; *Ipf1/Pdx1* and *Hlxb9* are expressed in β cells as they appear and are important for the expression of key β-cell genes (Ohlsson et al. 1993; Harrison et al. 1999; Li et al. 1999), whereas *Ptf1a* becomes restricted to differentiated acinar cells, where it regulates the expression of acinar enzymes (Krapp et al. 1996,1998; Li et al. 1999). qRT-pCR analyses revealed the expression of *IPF1*, *HLXB9*, and *PTF1A* in the developing human pancreas from 7 to 21 weeks (Figure 4A).

Immunohistochemical analyses showed that IPF1 is expressed in the epithelial progenitor cells throughout the period from 7 to 21 weeks as well as in insulin-expressing cells as they appear (Figure 4B). IPF1 expres-

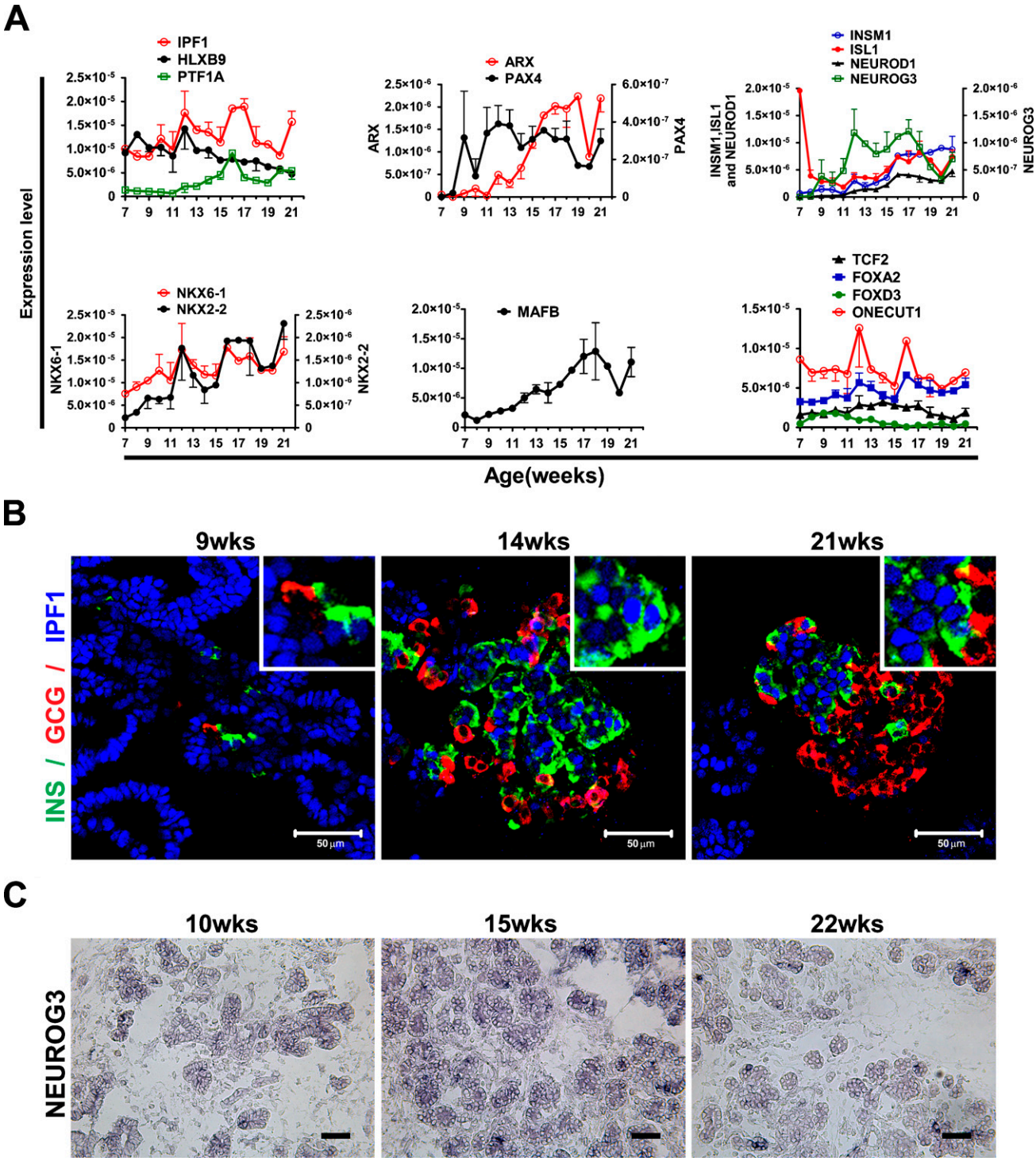

Figure 4 Expression of transcription factors in human fetal pancreas between weeks 7 and 21. (**A**) Expression analysis by quantitative real-time (qRT)-PCR of *HLXB9*, *IPF1*, *PTF1A*, *PAX4*, *ARX*, *NGN3*, *INSM1*, *ISL1*, *NEUROD1*, *NKX6-1*, *NKX2-2*, *MAFB TCF2*, *FOXA2*, *FOXD3*, and *ONECUT1*. (**B**) Immunostaining of 9-, 14-, and 21-week fetal pancreas using anti-insulin (green), anti-glucagon (red), and anti-IPF1 (blue) antibodies. Inserts show a higher magnification. (**C**) In situ hybridization analysis of the NGN3 spatial expression in 10-, 15-, and 22-week human fetal pancreas. Bar = 50 μm.

sion could also be observed in occasional glucagon-expressing cells at early but not at later stages of development (data not shown). The expression of IPF1 in glucagon-expressing cells appeared, however, weaker than that observed in pancreatic progenitor cells or insulin-expressing cells (Figure 4B). Although other studies have described a cytoplasmic localization of IPF1 in human fetal pancreas (Piper et al. 2004; Sarkar et al. 2008), we consistently observed a nuclear localization of IPF1 in all of the tissues and stages analyzed (Figure 4B).

The relative expression of the proendocrine gene *NGN3* (Gasa et al. 2004) was low prior to 9 weeks, but from 9 weeks onward, the expression increased sharply and remained high until 17 weeks, after which the expression declined (Figure 4A). In situ hybridization analysis further demonstrated that NGN3-expressing cells were present at all stages analyzed (Figure 4C). As expected, the relative expression of the differentiated endocrine cell markers *ISL1*, *NEUROD1*, and *INSM1* (Ahlgren et al. 1997; Naya et al. 1997; Gierl et al. 2006) was initially low but increased from week 15 onward (Figure 4A). Thus, as in mouse, the expression of the proendocrine gene *NGN3* precedes that of transcription factors linked to terminal endocrine cell differentiation (Gradwohl et al. 2000; Gu et al. 2002; Johansson et al. 2007). Similar to that observed in the mouse, Isl1 is expressed both in differentiated endocrine cells (Figure 5 and data not shown) as well as early pancreatic mesenchymal cells (Figure 5).

The expression of *PAX4*, which in mouse initially marks endocrine progenitors (Greenwood et al. 2007) and later β-cell progenitors (Collombat et al. 2003, 2005), and *ARX*, which in mouse marks α-cell progenitors (Collombat et al. 2003,2005), were virtually undetectable at 7 and 8 weeks (Figure 4A). By 9 weeks onward, *PAX4* expression was prominent, whereas *ARX* expression started to increase first after 11 weeks (Figure 4A). *NKX2.2* and *NKX6.1* expression was detectable at 7 weeks, and the expression of both transcription factors increased throughout the developmental stages analyzed (Figure 4A). *MAFB* expression also increased from 7 to 21 weeks, whereas the expression of *MAFA*, a marker for mature β cells, was virtually undetectable at all stages analyzed (Figure 4A and data not shown). Other factors linked to pancreatic cell specification and/or differentiation, such as the MODY5 gene *TCF2* (also known as *HNF1β*), *FOXA2*, *FOXD3*, and *ONECUT/HNF6*, were relatively highly expressed from week 7 until week 21 (Figure 4A).

Expression of Signaling Molecules and Growth Factors in the Developing Human Pancreas

We next analyzed the expression of genes encoding growth factors and signaling molecules involved in pancreatic progenitor cell proliferation and differentiation. First, we analyzed by qRT-PCR the expression of EGF receptor (*EGFR*) and FGF receptor 2 (*FGFR2*). The EGF and FGF signaling pathways are implicated in the growth and proliferation of pancreatic progenitor cells; *FGFR2B* (Revest et al. 2001) and *FGF10* (an FGFR2b high-affinity ligand) (Ohuchi et al. 2000; Bhushan et al. 2001) knockout mice show pancreatic hypoplasia. *EGFR* mutant mice show a pancreatic epithelial cell proliferation defect, a delay in β-cell generation, and perturbed islet cell migration (Miettinen et al. 2000). In the developing human pancreas, the expression of both receptors is high at 7 weeks but declines and is low from 11 weeks onward (Figure 6A).

During mouse pancreatic development, NOTCH signaling controls pancreatic cell differentiation (Apelqvist et al. 1999; Jensen et al. 2000), and qRT-PCR analyses revealed the expression of several NOTCH signaling components in the developing human pancreas. *NOTCH1* expression was high at 7 weeks but then declined, whereas the expression of *DELTA-LIKE-1* (*DLLK1*) was low until 11 weeks and then increased (Figure 6A). During the 7- to 21-week period, *HES1*, but not *HES5* or *HEY1*, was prominently expressed, although the expression levels gradually decreased from 7 to 21 weeks (Figure 6A).

Bone morphogenetic protein (BMP) 4 has been implicated in pancreatic endocrine progenitor cell expansion and inhibition of differentiation through ID2 (Hua et al. 2006). Moreover, BMP4 appears to be required for the acquisition and/or maintenance of β-cell function (Goulley et al. 2007). In the human fetal pancreas, *BMP4* and its type 1 receptor, *BMPR1A*, were expressed between 7 and 21 weeks (Figure 6A); the expression levels decreased sharply from 7 to 11 weeks and increased slightly from 11 to 21 weeks. Interestingly, *BMP4* and *ID2* showed similar expression profiles between 7 and 13 weeks, but whereas *ID2* expression remained low until 21 weeks, *BMP4* expression increased (Figure 6A).

Expression of Differentiated Endocrine and Exocrine Genes

qRT-PCR and immunostaining were performed to determine the expression profiles of markers for differentiated pancreatic endocrine cells. qRT-PCR analysis showed that upon an exponential-like increase in the expression of the endocrine hormones (Figure 6B), *GLUCAGON* (*GCG*), *INSULIN* (*INS*), and *SOMATOSTATIN* (*SST*) expression had increased 13,000, 7300 and 840-fold, respectively, at 18 weeks, as compared with that observed at 7 weeks. *GHRELIN* (*GHRL*) expression was considerably lower at all stages analyzed (Figure 6B). The expression of the islet amyloid polypeptide (*IAPP*) was virtually undetectable until

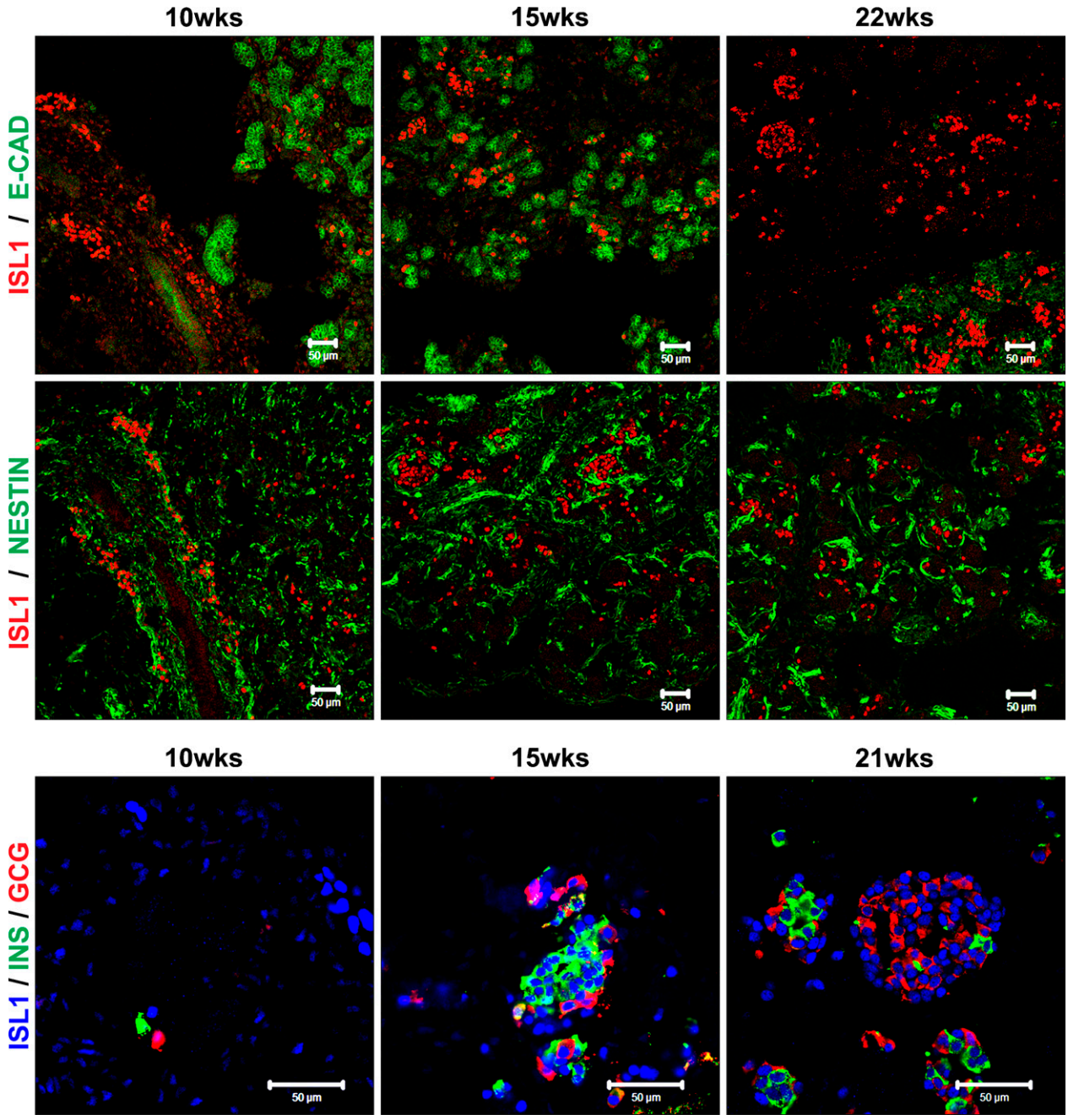

Figure 5 Isl1 expression during human pancreas development. Immunostaining of 10-, 15-, 21-, and 22-week fetal human pancreas using anti-Isl1 (red) and E-cadherin (green) (upper images), anti-Isl1 (red) and nestin (green) (middle images), and anti-Isl1 (blue), insulin (green), and glucagon (red) (lower images) antibodies. Bar = 50 μm.

week 17, but then increased dramatically, and the expression of *GLUCOKINASE* (*GCK*), the rate-limiting enzyme in glucose metabolism, increased 150-fold from 7 to 21 weeks, whereas glucose transporter type 2 (*GLUT2* or *SLC2A2*) expression was barely detectable at all stages analyzed (data not shown). The expression of the prohormone convertases *PCSK1* and *PCSK2* was initially low but increased 100- and 10-fold, respectively, from 11 weeks onward (Figure 6B). Finally, we analyzed the expression of ductal and acinar markers in the human fetal pancreas. The expression of carbonic anhydrase 2 (*CA2*), a marker for ductal cells, decreased 10-fold between 7 and 11 weeks, but then increased 13-fold between weeks 13 to 21 (Figure 6B). The expression of the acinar enzyme *AMYLASE* (*AMY*) was low throughout the period from 7 to 21 weeks

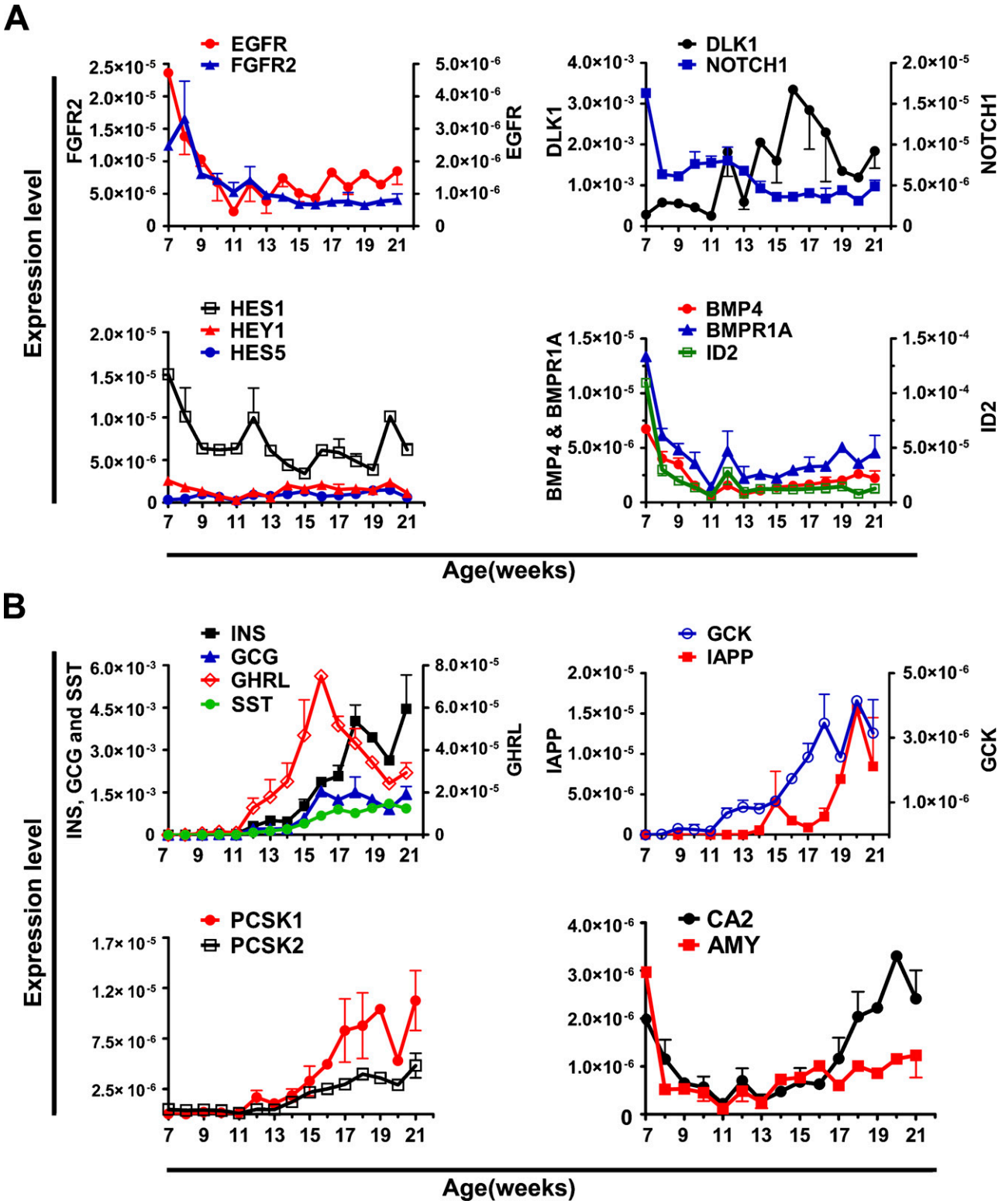

Figure 6 Expression of signaling molecules, growth factors, and endocrine markers in human fetal pancreas between weeks 7 and 21. Expression analysis by qRT-PCR of (**A**) *EGFR*, *FGFR2*, *DLLK1*, *NOTCH1*, *HES1*, *HES5*, *HEY1*, *BMP4*, *BMPR1A*, and *ID2*, and (**B**) *INS*, *GCG*, *SST*, *GHRL*, *GCK*, *IAPP*, *PCSK1*, *PCSK2*, *CA2*, and *AMY* in human fetal pancreas between 7 and 21 weeks of gestational age. Expression values are normalized with *18S*. Each data point is the mean ± SEM of one to three different specimens.

(Figure 6B) and undetectable by immunohistochemistry (data not shown).

Discussion

One of the most promising approaches to alleviating the lack of pancreatic donors needed for cell transplantation–based therapy is the generation of new insulin-producing cells, either from hES cells or embryonic pancreatic progenitor cells. Human stem cells represent a promising alternative source of insulin-producing cells, and recent reports by Baetge and coworkers (D'Amour et al. 2006; Kroon et al. 2008) have described encouraging protocols aiming to generate β cells in vitro from hES cells. These protocols failed, however, to produce fully mature β cells in vitro and resulted in the generation of cells equivalent to immature, fetal islet or pancreatic progenitor cells that required further development in vivo to generate glucose-responsive, insulin-producing cells capable of reversing diabetes in streptozotocin-treated mice (Kroon et al. 2008). Hence, increased knowledge regarding molecular mechanisms regulating the generation and maturation of human islets during normal development is critical for further improvements of these in vitro differentiation protocols. Animal models, in particular mouse, have been extensively used to study pancreatic developmental processes, and the results obtained are frequently extrapolated to the human pancreas. Recent studies (Brissova et al. 2005; Cabrera et al. 2006) have, however, demonstrated that differences between human and mouse islet cytoarchitecture have functional implications, stressing the necessity of fully deciphering human fetal islet development.

In this study, we have performed immunohistochemical analyses, examined the morphology of the forming islets, and analyzed the coexpression of insulin and glucagon during the period of hormone expression and islet clustering. Our study also includes sequential gene expression profile analyses of 36 human fetal pancreases, from 7 to 21 weeks, thus linking gene expression to organogenesis. The immunohistochemical analyses show that insulin- and glucagon-positive cells initially appear scattered within the pancreas, but by week 14, a characteristic structure with the insulin-positive cells in the center and the glucagon-positive cells in the periphery was apparent (Figure 1A). Next, the ring of glucagon-positive cells surrounding the core of insulin-positive cells appeared to "open up," and later, insulin- and glucagon-positive cells had expanded and now formed insulin cell and glucagon cell homogeneous clusters, respectively. Figure 1 shows images representative of the most advanced cell clusters, but at each stage, it is possible to find less-aggregated and single cells, mostly dependent on their intra-organ localization (Figure 3A). Figure 3B shows a schematic summary of the islet-like cluster formation that we observed through our immunohistochemical analyses of the fetal pancreas. The complete determination of the sequence of events that ultimately results in the formation of the typical adult human islet with intermingled insulin and glucagon cells would, however, require the analyses of fetal stages beyond weeks 21–22. Our results imply, however, that the process leading to the formation of mature human islets with intermingled β and α cells (Figure 1A) (Cabrera et al. 2006) occurs after 21 weeks of gestation. The mechanism and factors involved in the final organization of human islets remain unknown but are expected to involve cell migration events. Studies on the expression of various adhesion molecules during this period are likely to provide further insight into the process involved in the formation of mature human islets.

In agreement with previous observations (Bocian-Sobkowska et al. 1999), our immunohistochemical analyses revealed occasional insulin and glucagon double-positive cells, predominantly at early stages (Figure 2A). We also quantified the relative and absolute values of glucagon and insulin coexpression in human fetal pancreas from 8 to 21 weeks of gestational age (Figures 2B–2D). The method used to quantify the double expression of insulin and glucagon, i.e., the Zeiss LSM510 software (version 3.2), is based not on the visual observation of the change in color (i.e., from green and red to yellow), but on the measurement of light emission at different wavelengths within the same point, which makes the results more accurate and reproducible. The low number of cells coexpressing insulin and glucagon is constant from 10 to 21 weeks, although the relative number decreases. These results suggest that in the human developing pancreas, a small subfraction of immature endocrine cells may express more than one hormone, at least until week 21. At all stages analyzed, cells coexpressing insulin and glucagon are mainly restricted to small aggregates, suggesting that they represent newly formed endocrine cells.

Another interesting observation is that islet cell aggregation is heterogeneous within the developing pancreas; thus, it appears to initiate at the center of the tissue and then spread toward the periphery (Figure 3A), confirming previous studies (Polak et al. 2000). This observation suggests that endocrine cells are formed at the central region of the developing pancreas and migrate toward the periphery of the organ, where they start to cluster or, alternatively, that endocrine cells are continuously generated from progenitor cells present in the expanding ductal epithelium.

IPF1/Pdx1 plays an important role both during early pancreatic development and in adult β cells of both mice and men (Ohlsson et al. 1993; Jonsson et al. 1994; Offield et al. 1996; Stoffers et al. 1997a,b; Edlund 2001). Consistent with this dual role for *IPF1*, and in agreement with that seen during mouse pancreatic

development, we observed strong nuclear IPF1 expression in both early pancreatic progenitor cells and emerging β cells of human fetal pancreas. Although some studies have described a cytoplasmic location of IPF1 (Piper et al. 2004; Sarkar et al. 2008) and attributed a regulatory function to a presumed shuttling from the nucleus to the cytoplasm (Piper et al. 2004), we consistently observe a nuclear localization for IPF1 at all analyzed stages of human and mouse pancreatic development. From our experience, the procedure of fixation is critical in this respect because poor fixation leads to leakage of nuclear factors, including IPF1, to the cytoplasm.

The period of islet cell differentiation and clustering coincides with the expression of *NGN3*. In fact, the appearance of endocrine cell aggregates occurs simultaneously with the exponential increase in the expression of insulin and other hormones. At this point, our results differ from those reported by Lyttle et al. (2008). Thus, whereas they showed the *NGN3* expression level slightly declining from 8 to 21 weeks, we show a Gaussian distribution-like gene expression profile of *NGN3*. The fact that we performed our qRT-PCR analyses using samples from each individual gestational week from 8 to 21, whereas they pooled their samples in three groups (8–10 weeks, 14–16 weeks, and 19–21 weeks) may explain this difference. Our results suggest that similar to mouse and as hypothesized by others (Sarkar et al. 2008), a secondary transition that lasts for weeks, rather than days, occurs also during human pancreatic development.

In the developing mouse pancreas, *Isl1* is required independently for the formation of the dorsal pancreatic mesenchyme, and hence, dorsal pancreatic growth, as well as for islet cell differentiation (Ahlgren et al. 1997). Here we show that Isl1 is abundantly expressed in both early pancreatic mesenchymal cells and differentiated endocrine cells as they appear also in the human developing pancreas. This expression pattern suggests that Isl1 function is conserved from mice to humans.

The expression of *PAX4* and *ARX*, that defines the β- and α-cell fate, respectively (Collombat et al. 2003, 2005) is evident already at 7 weeks, but whereas *PAX4* expression increases rapidly between 7 and 13 weeks, *ARX* expression increases first after week 13. This differential expression of *PAX4* and *ARX* may in part explain why, in contrast to mouse pancreatic development, insulin-expressing cells appear earlier than glucagon-expressing cells during human pancreatic development, and why insulin-positive cells initially outnumber glucagon-positive cells. The developmental significance, if any, of the earlier appearance of insulin-positive cells in the developing human pancreas, as compared with mouse pancreas, is unclear. The expression of the retinoic acid–synthesizing enzyme *RALDH1* coincides, however, with the appearance of insulin-positive cells in both mouse and humans, and retinoic acid has been shown to positively influence β-cell differentiation from mouse pancreatic progenitor cells (Ostrom et al. 2008).

Previous studies have shown that fetal β cells are non-functional, i.e., they do not respond to glucose (Hoffman et al. 1982; Tuch et al. 1990). In agreement with those studies, the insulin-positive cells formed during the period analyzed do not express the mature β-cell marker *MAFA* (Nishimura et al. 2006), although other β-cell markers, such as *GCK*, *IAPP*, *PCSK1*, and *PCSK2* are expressed. The homotypic nature of the endocrine cell clusters at 18–21 weeks of gestation further strengthens the notion that the islet cells are immature at this stage.

In summary, we present here a detailed analysis of the morphological changes that occur during human pancreatic islet formation and the concomitant gene expression profiles of key markers during endocrine pancreas ontogeny. The data presented here may contribute to a better understanding of human islet formation and thus to the design of protocols aimed at generating insulin-producing cells, or islets, from human stem or progenitor cells for cell replacement therapies.

Acknowledgments

This work was supported by a grant from the Stanley Glaser Foundation (to JAD) and the Diabetes Research Institute Foundation (diabetesresearch.org).

We thank Kevin Johnson, George MacNamara, and Ainhoa Martin-Pagola for technical assistance, the Human Islet Cell Processing Facility at the Diabetes Research Institute, University of Miami, for providing the human adult pancreatic tissue, and Karen Bookbinder and Dr. Gerald Applegate for assistance with human fetal tissue procurement.

Literature Cited

Ahlgren U, Pfaff SL, Jessell TM, Edlund T, Edlund H (1997) Independent requirement for ISL1 in formation of pancreatic mesenchyme and islet cells. Nature 385:257–260

Apelqvist A, Li H, Sommer L, Beatus P, Anderson DJ, Honjo T, Hrabe de Angelis M, et al. (1999) Notch signalling controls pancreatic cell differentiation. Nature 400:877–881

Bhushan A, Itoh N, Kato S, Thiery JP, Czernichow P, Bellusci S, Scharfmann R (2001) Fgf10 is essential for maintaining the proliferative capacity of epithelial progenitor cells during early pancreatic organogenesis. Development 128:5109–5117

Bocian-Sobkowska J, Zabel M, Wozniak W, Surdyk-Zasada J (1999) Polyhormonal aspect of the endocrine cells of the human fetal pancreas. Histochem Cell Biol 112:147–153

Bonal C, Herrera PL (2008) Genes controlling pancreas ontogeny. Int J Dev Biol 52:823–835

Brissova M, Fowler MJ, Nicholson WE, Chu A, Hirshberg B, Harlan DM, Powers AC (2005) Assessment of human pancreatic islet architecture and composition by laser scanning confocal microscopy. J Histochem Cytochem 53:1087–1097

Cabrera O, Berman DM, Kenyon NS, Ricordi C, Berggren PO, Caicedo A (2006) The unique cytoarchitecture of human pancreatic islets has implications for islet cell function. Proc Natl Acad Sci USA 103:2334–2339

Collombat P, Hecksher-Sorensen J, Broccoli V, Krull J, Ponte I, Mundiger T, Smith J, et al. (2005) The simultaneous loss of Arx and Pax4 genes promotes a somatostatin-producing cell fate spec-

ification at the expense of the alpha- and beta-cell lineages in the mouse endocrine pancreas. Development 132:2969–2980
Collombat P, Mansouri A, Hecksher-Sorensen J, Serup P, Krull J, Gradwohl G, Gruss P (2003) Opposing actions of Arx and Pax4 in endocrine pancreas development. Genes Dev 17:2591–2603
D'Amour KA, Bang AG, Eliazer S, Kelly OG, Agulnick AD, Smart NG, Moorman MA, et al. (2006) Production of pancreatic hormone-expressing endocrine cells from human embryonic stem cells. Nat Biotechnol 24:1392–1401
Edlund H (1998) Transcribing pancreas. Diabetes 47:1817–1823
Edlund H (1999) Pancreas: how to get there from the gut? Curr Opin Cell Biol 11:663–668
Edlund H (2001) Factors controlling pancreatic cell differentiation and function. Diabetologia 44:1071–1079
Edlund H (2002) Pancreatic organogenesis: developmental mechanisms and implications for therapy. Nat Rev Genet 3:524–532
Gasa R, Mrejen C, Leachman N, Otten M, Barnes M, Wang J, Chakrabarti S, et al. (2004) Proendocrine genes coordinate the pancreatic islet differentiation program in vitro. Proc Natl Acad Sci USA 101:13245–13250
Gierl MS, Karoulias N, Wende H, Strehle M, Birchmeier C (2006) The zinc-finger factor Insm1 (IA-1) is essential for the development of pancreatic beta cells and intestinal endocrine cells. Genes Dev 20:2465–2478
Goulley J, Dahl U, Baeza N, Mishina Y, Edlund H (2007) BMP4-BMPR1A signaling in beta cells is required for and augments glucose-stimulated insulin secretion. Cell Metab 5:207–219
Gradwohl G, Dierich A, LeMeur M, Guillemot F (2000) Neurogenin3 is required for the development of the four endocrine cell lineages of the pancreas. Proc Natl Acad Sci USA 97:1607–1611
Greenwood AL, Li S, Jones K, Melton DA (2007) Notch signaling reveals developmental plasticity of Pax4(+) pancreatic endocrine progenitors and shunts them to a duct fate. Mech Dev 124:97–107
Gu G, Dubauskaite J, Melton DA (2002) Direct evidence for the pancreatic lineage: NGN3+ cells are islet progenitors and are distinct from duct progenitors. Development 129:2447–2457
Harrison KA, Thaler J, Pfaff SL, Gu H, Kehrl JH (1999) Pancreas dorsal lobe agenesis and abnormal islets of Langerhans in Hlxb9-deficient mice. Nat Genet 23:71–75
Hoffman L, Mandel TE, Carter WM, Koulmanda M, Martin FI (1982) Insulin secretion by fetal human pancreas in organ culture. Diabetologia 23:426–430
Hua H, Zhang YQ, Dabernat S, Kritzik M, Dietz D, Sterling L, Sarvetnick N (2006) BMP4 regulates pancreatic progenitor cell expansion through Id2. J Biol Chem 281:13574–13580
Jensen J, Pedersen EE, Galante P, Hald J, Heller RS, Ishibashi M, Kageyama R, et al. (2000) Control of endodermal endocrine development by Hes-1. Nat Genet 24:36–44
Johansson KA, Dursun U, Jordan N, Gu G, Beermann F, Gradwohl G, Grapin-Botton A (2007) Temporal control of neurogenin3 activity in pancreas progenitors reveals competence windows for the generation of different endocrine cell types. Dev Cell 12: 457–465
Jonsson J, Carlsson L, Edlund T, Edlund H (1994) Insulin-promoter-factor 1 is required for pancreas development in mice. Nature 371:606–609
Krapp A, Knofler M, Frutiger S, Hughes GJ, Hagenbuchle O, Wellauer PK (1996) The p48 DNA-binding subunit of transcription factor PTF1 is a new exocrine pancreas-specific basic helix-loop-helix protein. EMBO J 15:4317–4329
Krapp A, Knofler M, Ledermann B, Burki K, Berney C, Zoerkler N, Hagenbuchle O, et al. (1998) The bHLH protein PTF1-p48 is essential for the formation of the exocrine and the correct spatial organization of the endocrine pancreas. Genes Dev 12:3752–3763
Kroon E, Martinson LA, Kadoya K, Bang AG, Kelly OG, Eliazer S, Young H, et al. (2008) Pancreatic endoderm derived from human embryonic stem cells generates glucose-responsive insulin-secreting cells in vivo. Nat Biotechnol 26:443–452
Li H, Arber S, Jessell TM, Edlund H (1999) Selective agenesis of the dorsal pancreas in mice lacking homeobox gene Hlxb9. Nat Genet 23:67–70
Lyttle BM, Li J, Krishnamurthy M, Fellows F, Wheeler MB, Goodyer CG, Wang R (2008) Transcription factor expression in the developing human fetal endocrine pancreas. Diabetologia 51:1169–1180
Miettinen PJ, Huotari M, Koivisto T, Ustinov J, Palgi J, Rasilainen S, Lehtonen E, et al. (2000) Impaired migration and delayed differentiation of pancreatic islet cells in mice lacking EGF-receptors. Development 127:2617–2627
Naya FJ, Huang HP, Qiu Y, Mutoh H, DeMayo FJ, Leiter AB, Tsai MJ (1997) Diabetes, defective pancreatic morphogenesis, and abnormal enteroendocrine differentiation in BETA2/neuroD-deficient mice. Genes Dev 11:2323–2334
Nishimura W, Kondo T, Salameh T, El Khattabi I, Dodge R, Bonner-Weir S, Sharma A (2006) A switch from MafB to MafA expression accompanies differentiation to pancreatic beta-cells. Dev Biol 293:526–539
Obernosterer G, Martinez J, Alenius M (2007) Locked nucleic acid-based in situ detection of microRNAs in mouse tissue sections. Nat Protocols 2:1508–1514
Offield MF, Jetton TL, Labosky PA, Ray M, Stein RW, Magnuson MA, Hogan BL, et al. (1996) PDX-1 is required for pancreatic outgrowth and differentiation of the rostral duodenum. Development 122:983–995
Ohlsson H, Karlsson K, Edlund T (1993) IPF1, a homeodomain-containing transactivator of the insulin gene. EMBO J 12:4251–4259
Ohuchi H, Hori Y, Yamasaki M, Harada H, Sekine K, Kato S, Itoh N (2000) FGF10 acts as a major ligand for FGF receptor 2 IIIb in mouse multi-organ development. Biochem Biophys Res Commun 277:643–649
Oliver-Krasinski JM, Stoffers DA (2008) On the origin of the beta cell. Genes Dev 22:1998–2021
Ostrom M, Loffler KA, Edfalk S, Selander L, Dahl U, Ricordi C, Jeon J, et al. (2008) Retinoic acid promotes the generation of pancreatic endocrine progenitor cells and their further differentiation into beta-cells. PLoS One 3:e2841
Piper K, Brickwood S, Turnpenny LW, Cameron IT, Ball SG, Wilson DI, Hanley NA (2004) Beta cell differentiation during early human pancreas development. J Endocrinol 181:11–23
Polak M, Bouchareb-Banaei L, Scharfmann R, Czernichow P (2000) Early pattern of differentiation in the human pancreas. Diabetes 49:225–232
Revest JM, Spencer-Dene B, Kerr K, De Moerlooze L, Rosewell I, Dickson C (2001) Fibroblast growth factor receptor 2-IIIb acts upstream of Shh and Fgf4 and is required for limb bud maintenance but not for the induction of Fgf8, Fgf10, Msx1, or Bmp4. Dev Biol 231:47–62
Sarkar SA, Kobberup S, Wong R, Lopez AD, Quayum N, Still T, Kutchma A, et al. (2008) Global gene expression profiling and histochemical analysis of the developing human fetal pancreas. Diabetologia 51:285–297
Stoffers DA, Ferrer J, Clarke WL, Habener JF (1997a) Early-onset type-II diabetes mellitus (MODY4) linked to IPF1. Nat Genet 17:138–139
Stoffers DA, Zinkin NT, Stanojevic V, Clarke WL, Habener JF (1997b) Pancreatic agenesis attributable to a single nucleotide deletion in the human IPF1 gene coding sequence. Nat Genet 15:106–110
Tuch BE, Osgerby KJ, Turtle JR (1990) The role of calcium in insulin release from the human fetal pancreas. Cell Calcium 11:1–9

The Journal of Histochemistry & Cytochemistry